

- ⁹ Duke University, Durham, North Carolina 27708
¹⁰ Fermi National Accelerator Laboratory, Batavia, Illinois 60510
¹¹ University of Florida, Gainesville, Florida 32611
¹² Laboratori Nazionali di Frascati, Istituto Nazionale di Fisica Nucleare, I-00044 Frascati, Italy
¹³ University of Geneva, CH-1211 Geneva 4, Switzerland
¹⁴ Harvard University, Cambridge, Massachusetts 02138
¹⁵ Hiroshima University, Higashi-Hiroshima 724, Japan
¹⁶ University of Illinois, Urbana, Illinois 61801
¹⁷ The Johns Hopkins University, Baltimore, Maryland 21218
¹⁸ Institut für Experimentelle Kernphysik, Universität Karlsruhe, 76128 Karlsruhe, Germany
¹⁹ Korean Hadron Collider Laboratory: Kyungpook National University, Taegu 702-701; Seoul National University, Seoul 151-742; and SungKyunKwan University, Suwon 440-746; Korea
²⁰ National Laboratory for High Energy Physics (KEK), Tsukuba, Ibaraki 305, Japan
²¹ Ernest Orlando Lawrence Berkeley National Laboratory, Berkeley, California 94720
²² Massachusetts Institute of Technology, Cambridge, Massachusetts 02139
²³ Institute of Particle Physics: McGill University, Montreal H3A 2T8; and University of Toronto, Toronto M5S 1A7; Canada
²⁴ University of Michigan, Ann Arbor, Michigan 48109
²⁵ Michigan State University, East Lansing, Michigan 48824
²⁶ University of New Mexico, Albuquerque, New Mexico 87131
²⁷ The Ohio State University, Columbus, Ohio 43210
²⁸ Osaka City University, Osaka 588, Japan
²⁹ Universita di Padova, Istituto Nazionale di Fisica Nucleare, Sezione di Padova, I-35131 Padova, Italy
³⁰ University of Pennsylvania, Philadelphia, Pennsylvania 19104
³¹ Istituto Nazionale di Fisica Nucleare, University and Scuola Normale Superiore of Pisa, I-56100 Pisa, Italy
³² University of Pittsburgh, Pittsburgh, Pennsylvania 15260
³³ Purdue University, West Lafayette, Indiana 47907
³⁴ University of Rochester, Rochester, New York 14627
³⁵ Rockefeller University, New York, New York 10021
³⁶ Rutgers University, Piscataway, New Jersey 08855
³⁷ Texas A&M University, College Station, Texas 77843
³⁸ Texas Tech University, Lubbock, Texas 79409
³⁹ Istituto Nazionale di Fisica Nucleare, University of Trieste/ Udine, Italy
⁴⁰ University of Tsukuba, Tsukuba, Ibaraki 305, Japan
⁴¹ Tufts University, Medford, Massachusetts 02155
⁴² Waseda University, Tokyo 169, Japan
⁴³ University of Wisconsin, Madison, Wisconsin 53706
⁴⁴ Yale University, New Haven, Connecticut 06520

Abstract

We report on a search for the flavor-changing neutral current decays $B^+ \rightarrow \mu^+ \mu^- K^+$ and $B^0 \rightarrow \mu^+ \mu^- K^{*0}$ using 88 pb⁻¹ of data from $\bar{p}p$ collisions at

$\sqrt{s} = 1.8$ TeV, collected with the Collider Detector at Fermilab. Finding no evidence for these decays, we set upper limits on the branching fractions $\mathcal{B}(B^+ \rightarrow \mu^+ \mu^- K^+) < 5.2 \times 10^{-6}$ and $\mathcal{B}(B^0 \rightarrow \mu^+ \mu^- K^{*0}) < 4.0 \times 10^{-6}$ at the 90% confidence level.

13.25.Hw, 13.30.Ce

In the Standard Model of electroweak interactions, the flavor-changing neutral current (FCNC) processes $B^+ \rightarrow \mu^+\mu^-K^+$ and $B^0 \rightarrow \mu^+\mu^-K^{*0}$ [1] are forbidden at tree level. At higher order, these decays occur through penguin and box diagrams with predicted branching fractions $(0.3 - 0.5) \times 10^{-6}$ for $B^+ \rightarrow \mu^+\mu^-K^+$ and $(1.0 - 1.5) \times 10^{-6}$ for $B^0 \rightarrow \mu^+\mu^-K^{*0}$ [2]. Many deviations from Standard Model physics, such as charged Higgs bosons or anomalous W couplings, can increase these rates significantly [3]. Because the spread in Standard Model predictions, due mainly to uncertainties in hadronic form factors, is well bounded, the observation of much larger branching fractions would be a signal for physics outside the Standard Model.

To date, no observation of these decays has been reported. The CLEO collaboration [4] has set the limits $\mathcal{B}(B^+ \rightarrow \mu^+\mu^-K^+) < 0.97 \times 10^{-5}$ and $\mathcal{B}(B^0 \rightarrow \mu^+\mu^-K^{*0}) < 0.95 \times 10^{-5}$ at the 90% confidence level (C.L.). The CDF collaboration [5] has previously searched for these decays in an 18 pb^{-1} data sample recorded in 1992-1993 and set the 90% C.L. limits $\mathcal{B}(B^+ \rightarrow \mu^+\mu^-K^+) < 1.0 \times 10^{-5}$ and $\mathcal{B}(B^0 \rightarrow \mu^+\mu^-K^{*0}) < 2.5 \times 10^{-5}$. The result presented in this Letter is based on an 88 pb^{-1} combined data sample from the 1992-1993 and 1994-1995 running periods and supersedes the earlier CDF result.

Briefly, the method used in this search is as follows. The CDF trigger selects events containing two muon candidates, which we combine offline with K^+ and K^{*0} candidates to form B^+ and B^0 candidates. Using the topologically identical resonant processes $B^+ \rightarrow J/\psi K^+ \rightarrow (\mu^+\mu^-)K^+$ and $B^0 \rightarrow J/\psi K^{*0} \rightarrow (\mu^+\mu^-)K^{*0}$ for normalization, we measure ratios of branching fractions, thus canceling most uncertainties due to B meson production and detection efficiency. Small acceptance and trigger efficiency differences due to the different decay kinematics are corrected with a Monte Carlo calculation.

The CDF detector has been described in detail elsewhere [6]. Detector components most relevant to this search are the muon chambers and charged particle tracking system. The muon system is composed of drift chambers outside the hadron calorimeter, allowing the reconstruction of track segments for penetrating particles in the pseudorapidity [7] range $|\eta| < 1$. The minimum transverse momentum (p_T) of detectable muons varies between 1.4 and 2.2 GeV/ c as a function of η , depending on the amount of material between the interaction point and the muon chambers. Charged particles are reconstructed in the central tracking chamber (CTC) and the silicon vertex detector (SVX) [8], both located inside a 1.4 T solenoidal magnetic field. The CTC, covering $|\eta| < 1.1$, is a cylindrical drift chamber containing 84 layers grouped into nine alternating superlayers of axial and stereo wires. The SVX consists of four layers of single-sided silicon microstrip detectors mounted at radii between 2.9 and 7.9 cm from the beam. It provides track measurements in the $r\phi$ plane with impact parameter resolution $(13 + 40/p_T) \mu\text{m}$, where p_T is in GeV/ c . The impact parameter of a track is defined as the distance of closest approach to the beam in a plane transverse to the beam.

CDF uses a three-level trigger system. The muon pair trigger requires the presence of two track segments in the muon chambers at the first level and matching CTC track candidates found by the central fast track processor (CFT) [9] for one or both muon segments at the second level. The third-level trigger tightens the matching criteria using fully reconstructed CTC tracks.

Muons inside the acceptance of the muon chambers are found by the first-level trigger with an efficiency that rises from about 40% at $p_T = 1.5 \text{ GeV}/c$ to a plateau value of 93% for

muon transverse momenta exceeding $3 \text{ GeV}/c$. The efficiency for finding the corresponding tracks with the CFT at level two rises from about 50% at $p_T = 2 \text{ GeV}/c$ to about 96% for $p_T > 2.3 \text{ GeV}/c$. If one muon does not have a matching CFT track a higher p_T threshold is imposed for the other muon, leading to an efficiency that rises from about 50% at $p_T = 2.6 \text{ GeV}/c$ and reaches the same plateau value for $p_T > 3.1 \text{ GeV}/c$. The first type of trigger, requiring two CFT tracks, was not implemented during the 1992-1993 running period. A muon pair is called resonant when its invariant mass is close to the $c\bar{c}$ -resonances J/ψ or ψ' . Event selection is identical for resonant and non-resonant muon pairs.

To reconstruct $\mu^+\mu^-K^+$ candidates, we combine the two muon candidates selected by the trigger with an additional charged track, assumed to be a kaon. The kaon track must satisfy $p_T > 2 \text{ GeV}/c$, and the B candidate must satisfy $p_T > 6 \text{ GeV}/c$.

The reconstruction of the K^{*0} in the $B^0 \rightarrow \mu^+\mu^-K^{*0}$ process is via the $K^{*0} \rightarrow K^+\pi^-$ decay. We require $p_T > 0.5 \text{ GeV}/c$ for each track, and to reduce random combinations, we require $p_T > 2 \text{ GeV}/c$ for the K^{*0} candidate. To allow for the $K^*(892)^0$ width, we require the K^{*0} candidate mass to be between 796 and 996 MeV/c^2 . No particle identification is used, and each pair of tracks is considered as $K^+\pi^-$ and π^+K^- , respectively. We choose the K^{*0}/\bar{K}^{*0} -daughter mass assignment with invariant mass closer to the world-average K^{*0} mass.

An isolation requirement is a well established means of improving the signal to background ratio in reconstructing B decays. We require isolation $I > 0.6$, where I is the transverse momentum of the B candidate divided by the scalar sum of the transverse momenta of the B and all other tracks in a cone $\sqrt{(\Delta\eta)^2 + (\Delta\phi)^2} < 1.0$ around the B momentum. The measured efficiency from our data for the requirement $I > 0.6$ is $92 \pm 6\%$ for B mesons with $p_T > 6 \text{ GeV}/c$ and $|\eta| < 1$.

A possible background for the rare decay search comes from $B \rightarrow J/\psi K$ decays in which the kaon is misidentified as a muon and the muon is taken as the kaon instead. We apply a cut to remove candidates that are compatible with this hypothesis. In fact, no non-resonant candidate showed this ambiguity after all other selection cuts were applied.

We require B daughters to be consistent with originating at a displaced decay vertex and inconsistent with originating at the beam line. All tracks forming the B candidate must include hits on at least three SVX layers, to ensure a good impact parameter measurement, and must miss the beam line with at least 2σ significance, where σ is the estimated impact parameter resolution. The tracks are fit to a common decay vertex. The fit assumes that the B meson is produced at the beam line and constrains the B momentum to be parallel to its line of flight in the $r-\phi$ plane. The fit quality must be acceptable ($\chi^2 < 20$ with 4 degrees of freedom for $\mu^+\mu^-K^+$ and 6 for $\mu^+\mu^-K^{*0}$) and the transverse decay length must exceed $400 \mu\text{m}$. The transverse decay length is the distance between the beam line and the B decay vertex measured in the $r - \phi$ plane. The beam spot of the Tevatron has a transverse size of approximately $25 \mu\text{m}$ (R.M.S.) and a mean that is measured with negligible uncertainty [10]. The impact-parameter and decay-length criteria are chosen to minimize the expected upper limit using the signal efficiency from a Monte Carlo calculation and a background estimate from the B sideband mass region $5.38\text{--}5.88 \text{ GeV}/c^2$.

Figures 1 and 2 show scatter plots of the $\mu^+\mu^-K^+$ and $\mu^+\mu^-K^{*0}$ mass versus the $\mu^+\mu^-$ mass for candidates passing all requirements. The signal region for B mesons, whose half width is chosen to be twice the invariant mass resolution, includes reconstructed B meson

masses between 5.23 and 5.33 GeV/c^2 .

The decays $B^+ \rightarrow J/\psi(\psi')K^+$ and $B^0 \rightarrow J/\psi(\psi')K^{*0}$ followed by $J/\psi(\psi') \rightarrow \mu^+\mu^-$ have product branching fractions two orders of magnitude larger than the Standard Model predictions for the non-resonant $B^+ \rightarrow \mu^+\mu^-K^+$ and $B^0 \rightarrow \mu^+\mu^-K^{*0}$ decays. Candidates with an invariant mass of the muon pair in the regions 2.9–3.3 GeV/c^2 or 3.6–3.8 GeV/c^2 are therefore excluded from the rare decay search. Events that have dimuon masses within 100 MeV/c^2 of the J/ψ mass are used as the normalization sample.

In the B mass region for $\mu^+\mu^-K^+$ final states, we count 4 non-resonant candidates and count 122 J/ψ candidates. In case of the $\mu^+\mu^-K^{*0}$ final state, no non-resonant candidate is found in the B -mass region, while we count 76 J/ψ candidates. The background for the resonant decays is estimated by counting events in the B mass sideband 5.38 – 5.88 GeV/c^2 and scaling for the relative sizes of the B signal region and sideband regions. The estimates obtained this way are 0.4 events for $B^+ \rightarrow J/\psi K^+$ and 0.6 events for $B^0 \rightarrow J/\psi K^{*0}$.

The excess of resonant events in the sideband below the B signal region over the sideband above the B -mass is understood to come from incompletely reconstructed $B \rightarrow J/\psi X$ decays. The non-resonant excess below the B signal region is not understood. The high mass sideband, five times as wide as the signal region, contains 4 non-resonant $\mu^+\mu^-K^+$ and 2 non-resonant $\mu^+\mu^-K^{*0}$ candidates. Note that simply extrapolating these sideband rates may underestimate the background in the signal region, because the high-mass sideband is used to optimize the selection criteria.

Assuming all observed candidates in the signal region are signal events, we set upper limits on the numbers of observable FCNC decays using Poisson statistics and conclude that $\bar{N}(\mu^+\mu^-K^+) < 8.0$ and $\bar{N}(\mu^+\mu^-K^{*0}) < 2.3$ at the 90% confidence level.

We use a Monte Carlo simulation to calculate R_ϵ , the ratio of the total trigger and reconstruction efficiency for the non-resonant mode to that of the J/ψ mode, including the effect of the restricted dimuon mass range in the case of non-resonant decays. In the Monte Carlo simulation, B decays are sampled from a phase space distribution and weighted according to the decay amplitude, using form factors and Wilson coefficients taken from Ref. [11]. We find $R_\epsilon(\mu^+\mu^-K^+) = 0.79$ and $R_\epsilon(\mu^+\mu^-K^{*0}) = 0.65$. For observable numbers $\bar{N}(\mu^+\mu^-K^{(*)})$ and $\bar{N}(J/\psi K^{(*)})$ of non-resonant and J/ψ decays, one obtains the branching fractions for the FCNC decays,

$$\mathcal{B}(B \rightarrow \mu^+\mu^-K^{(*)}) = \frac{\bar{N}(\mu^+\mu^-K^{(*)})}{N(J/\psi K^{(*)}) \times R_\epsilon} \times \mathcal{B}(B \rightarrow J/\psi K^{(*)}) \times \mathcal{B}(J/\psi \rightarrow \mu^+\mu^-).$$

Whereas the central values of R_ϵ assume Standard Model couplings, distributions of kinematic variables in the decays $B \rightarrow \mu^+\mu^-K^{(*)}$ can be sensitive to non-standard short-distance interactions [11,12]. This affects the trigger efficiency, the acceptance of the event selection, and the extrapolation over excluded dimuon mass regions. To study such model dependence, we varied the signs of the relevant Wilson coefficients at M_W , as suggested in Ref. [11], and found the change in efficiency to be much less than the change in the predicted branching fraction. No variation in R_ϵ larger than 4% (12%) was found for $\mu^+\mu^-K^+$ ($\mu^+\mu^-K^{*0}$).

While this procedure does not cover the most general set of models, we conclude that the limits reported in this Letter, which are determined assuming Standard Model couplings, will change little when applied to many extended models. We do not treat model dependence as a source of error.

The impact of hadronic form factor uncertainties on R_ϵ was studied by replacing the form factors from Ref. [11] by the two sets given in Ref. [13]. We use the observed change in R_ϵ , less than 4% (8%) for the K (K^*) mode, as an estimate of the systematic error due to form factors.

Dominant systematic errors are the 11% (14%) uncertainty on the product of world average values for the branching fractions $B \rightarrow J/\psi K^+$ (K^{*0}) and $J/\psi \rightarrow \mu^+ \mu^-$ [14], and the statistical uncertainty on the number of resonant events. All other sources of error are found to make much smaller contributions. We estimate the total systematic error, including hadronic uncertainties, to be 15% (20%) for $\mu^+ \mu^- K(K^*)$, and include it in the determination of an upper limit on the branching fraction, using the method of Ref. [15].

Assuming all observed candidates to be signal events we find

$$\mathcal{B}(B^+ \rightarrow \mu^+ \mu^- K^+) < 5.2 \times 10^{-6}$$

and

$$\mathcal{B}(B^0 \rightarrow \mu^+ \mu^- K^{*0}) < 4.0 \times 10^{-6}$$

at 90% confidence level. These are the strictest limits on these decay branching fractions to date. Assuming Standard Model predictions, the expectation is to observe approximately 0.5 signal events in each channel.

We thank the Fermilab staff and the technical staffs of the participating institutions for their vital contributions. This work was supported by the U.S. Department of Energy and National Science Foundation, the Italian Istituto Nazionale di Fisica Nucleare; the Ministry of Education, Science and Culture of Japan, the Natural Sciences and Engineering Research Council of Canada, the National Science Council of the Republic of China, the A. P. Sloan Foundation, and the Alexander von Humboldt-Stiftung.

REFERENCES

- [1] Throughout this paper, reference to a decay mode implies the charge conjugate process as well.
- [2] A. Ali, Nucl. Phys. B, Proc. Suppl. **59**, 86 (1997); D. Melikhov, N. Nikitin and S. Simula, Phys. Rev. D**57**, 6814 (1998); T. M. Aliev, M. Savci and A. Özpineci, Phys. Rev. D**56**, 4260 (1996); P. Colangelo, F. De Fazio, P. Santorelli and E. Scrimieri, Phys. Rev. D**53**, 3672 (1996); C. Q. Geng and C. P. Kao, Phys. Rev. D**54**, 5636 (1996).
- [3] G. Burdman, Phys. Rev. D**59**, 035001 (1999); T. M. Aliev, M. Savci, A. Özpineci and I. L. Koru, Phys. Lett. B**410**, 216 (1997); N. G. Deshpande, K. Panose and J. Trampetic, Phys. Lett. B**308**, 322 (1993); Y. Okada, Y. Shimizu and M. Tanaka, Phys. Lett. B**405**, 297 (1997).
- [4] R. Godang *et al.*, CLEO CONF 98-22; to be published in *Proceedings of the XXVII International Conference on High Energy Physics*, Vancouver, Canada, 1998, edited by A. Astbury, D. Axen and J. Robinson (World Scientific, 1999).
- [5] F. Abe, *et al.*, Phys. Rev. Lett. **76**, 4675 (1996).
- [6] F. Abe *et al.*, Nucl. Instrum. Meth. A**271**, 387 (1988); F. Abe *et al.*, Phys. Rev. D**50**, 2966 (1994).
- [7] In CDF, the positive z axis lies along the proton direction, r is the radius from this axis, θ is the polar angle, and ϕ is the azimuthal angle. The pseudorapidity, η , is defined as $\eta = \ln \cot(\theta/2)$. Directions perpendicular to the z axis are called transverse.
- [8] D. Amidei *et al.*, Nucl. Instrum. Meth. A**350**, 73 (1994).
- [9] G.W. Foster, J. Freeman, C. Newman-Holmes, and J. Patrick, Nucl. Instr. Meth. A**269**, 93 (1988).
- [10] F. Abe *et al.*, Phys. Rev. D**57**, 5382 (1998).
- [11] C. Greub, A. Ioannissian and D. Wyler, Phys. Lett. B**346**, 149 (1995).
- [12] G. Burdman, Phys. Rev. D**52**, 6400 (1995).
- [13] D. Melikhov, N. Nikitin and S. Simula, Phys. Rev. D**57**, 6814 (1998).
- [14] C. Caso *et al.*, Eur. Jour. Phys C**3**, 1 (1998).
- [15] R. D. Cousins and V. L. Highland, Nucl. Instrum. Meth. A**320**, 331 (1992).

FIGURES

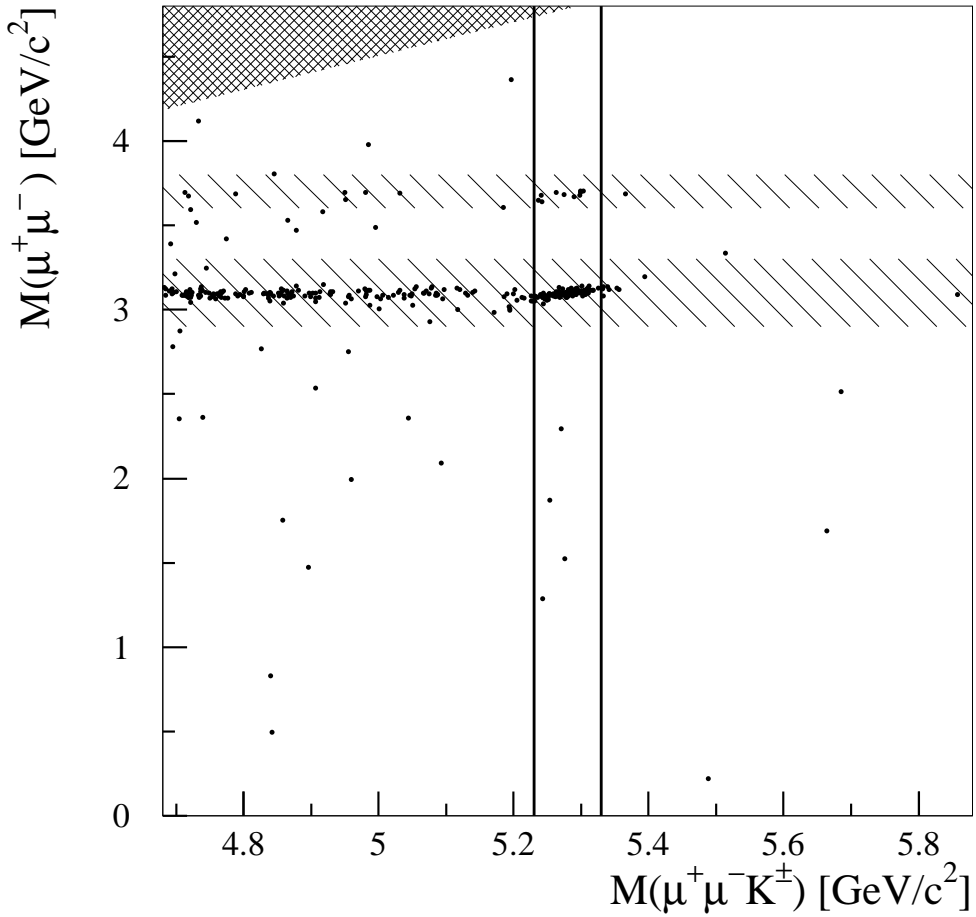


FIG. 1. Scatter plot showing the $B^\pm \rightarrow \mu^+\mu^-K^\pm$ candidates. The hatched horizontal bands are the excluded regions around the J/ψ and ψ' resonances. The signal region is between the vertical lines. The cross-hatched area in the upper left corner is kinematically forbidden. Entries with $M(\mu^+\mu^-K^\pm) < 5.23 \text{ GeV}/c^2$ and dimuon masses in the J/ψ region can be attributed to incompletely reconstructed $B \rightarrow J/\psi X$ decays.

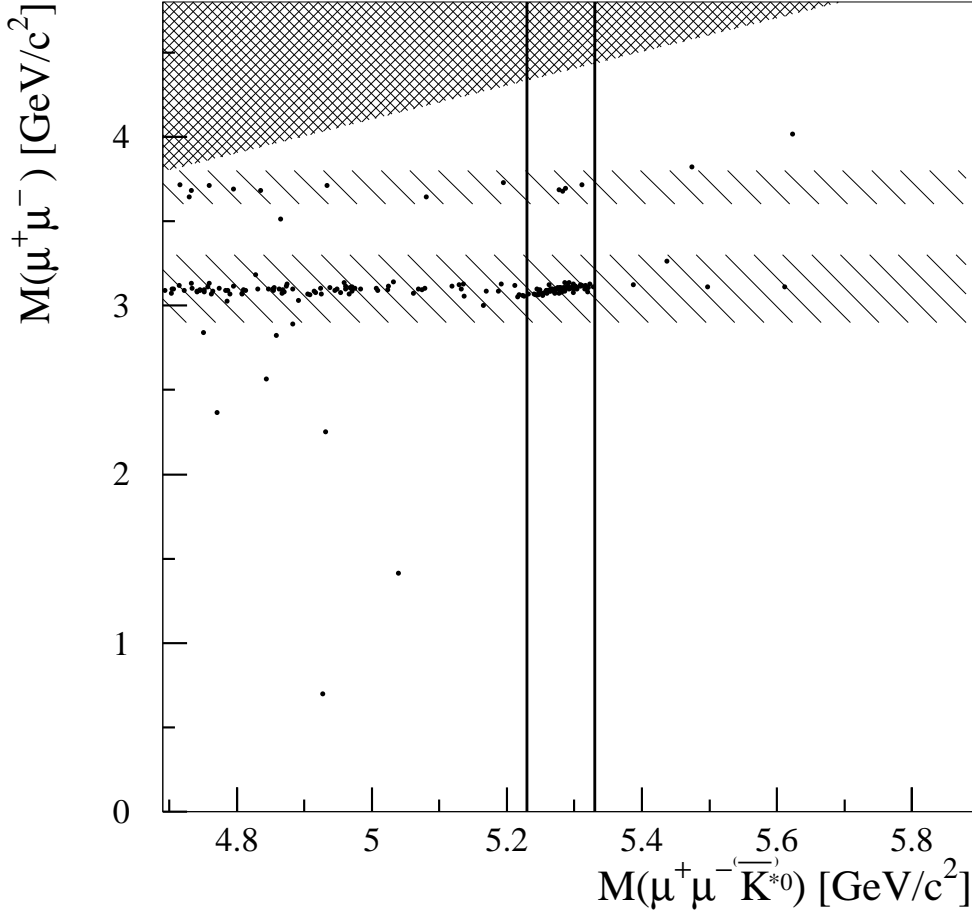


FIG. 2. Scatter plot showing the $B^0 \rightarrow \mu^+\mu^-K^{*0}$ and $\bar{B}^0 \rightarrow \mu^+\mu^-\bar{K}^{*0}$ candidates. The hatched horizontal bands are the excluded regions around the J/ψ and ψ' resonances.